Available online at www.sciencedirect.com
SCIENCE DIRECT®
International Journal of Pharmaceutics 279 (2004) 9–17
international journal of pharmaceutics
www.elsevier.com/locate/ijpharm

Shear distribution and variability in the USP Apparatus 2 under turbulent conditions

J. Kukura, J.L. Baxter, F.J. Muzzio*

Department of Chemical & Biochemical Engineering, Rutgers University, 98 Brett Road, Piscataway, NJ 08854, USA

Received 21 October 2003; received in revised form 19 March 2004; accepted 19 March 2004

Abstract

Computational analysis is used to examine the hydrodynamic environment within the USP Apparatus II at common operating conditions. Experimental validation of the computational model shows that the simulations of fluid motion match the dispersion of dye observed in experiments. The computations are then used to obtain data that cannot be easily measured with experiments, specifically the distribution of shear forces within the media and along the wall. Results show that the shear environment is highly non-uniform. Increasing the paddle speed from 50 to 100 rpm does not improve shear homogeneity within the apparatus. Experiments show that this uneven distribution of hydrodynamic forces is a direct cause of dissolution testing variability. This variability is large enough to cause for type II dissolution test failures, i.e., failures are a result of a vulnerability of the testing method rather than a problem with a dosage form. Future development of new dissolution tests should include evaluations of the hydrodynamic environments to eliminate this potential source of failure that is unrelated to product quality.

Keywords: Dissolution; Hydrodynamics; USP Apparatus 2; Tablet location; Shear; CFD

1. Introduction

In vitro drug dissolution testing is a critical component of pharmaceutical product and process development and manufacturing. Pharmaceutical scientists use it to guide formulation development and verify the consistency of the drug released from a dosage form. The two most common methods used for drug dissolution testing are the United States Pharmacopeia (USP) Basket Method (Apparatus I) and the USP Paddle Method (Apparatus II) (US Pharmacopeia XXIV, 2000).

Over the last 30 years, the FDA has emphasized the importance of drug dissolution testing in assuring lot-to-lot performance and bioequivalence of drugs. More recently, regulatory agencies have been suggesting implementing a larger role for dissolution testing, aimed at achieving accelerated approval and reducing the cost of bringing drug products to the market (Qureshi and Shabnam, 2001). However, despite the reliance of the industry and government on dissolution testing, the test itself is poorly understood and often produces inconsistent or inaccurate measurements. Failed dissolution tests resulted in fourteen product recalls in 1999 (18% of non-manufacturing recalls for oral solid dosage forms), and twenty product recalls in 2000 (24% of non-manufacturing recalls for oral solid

* Corresponding author. Tel.: +1 732 445 3357.
E-mail address: muzzio@sol.rutgers.edu (F.J. Muzzio).

0378-5173/$ – see front matter © 2004 Elsevier B.V. All rights reserved.
doi:10.1016/j.ijpharm.2004.03.033

dosage forms) (The Gold Sheet, 2000, 2001). The financial consequences of a failed dissolution test can be significant for a pharmaceutical corporation, necessitating product recalls, costly investigations, potential production delays and even revalidation of the manufacturing process. Compounding the problem, there have been numerous reports in the literature describing high variability and unpredictability of test results even for dissolution apparatus calibrator tablets (Cox et al., 1983; Moore et al., 1995, 1997; Qureshi and Shabnam, 2001).

Much of the uncontrolled variability typical of the dissolution test is likely the result of hydrodynamic effects since the test is conducted in a small agitated vessel operated at Reynolds numbers[1] in the transitional regime. Under such conditions, flow behavior in stirred tanks is known to be both time-dependent and strongly heterogeneous. Consequently, the hydrodynamics in the vicinity of a tablet in the dissolution device would likely be both position and time-dependent. Fluctuations in the flow introduce variability in the evolution of processes that are affected by hydrodynamics, such as shearing of the tablet surface, de-agglomeration of particles, mass transfer from the solid to the liquid, suspension and mixing of tablet fragments.

Hydrodynamics have been shown qualitatively to influence dissolution test performance for several decades. Studies published in the literature have shown that changes in the agitation speed can alter the measured dissolution rates and impact the ability to correlate in vitro dissolution tests with in vivo performance (Hamlin et al., 1962; Levy, 1963; Costa and Lobo, 2001). The hydrodynamic influences of geometrical changes, such as size and shape of the vessel and placement of sample probes, have also been examined (Qureshi and Shabnam, 2001; Underwood and Cadwallder, 1976; Cartensen et al., 1978; Wells, 1981; Beckett et al., 1996; Morihara et al., 2002). However, the majority of the previous work has focused on correlating operating conditions or configurations to dissolution rates but did not include a comprehensive analysis of the nature of the fluid motion. Only a few studies have been reported in the literature focusing on evaluating the hydrodynamics of the fluid flow within the dissolution device. Vongvirat et al. performed visualization studies with dye released from a non-disintegrating tablet in a rotating basket apparatus to show that shear patterns can be unstable across the surface of a tablet (Vongvirat et al., 1981). They also explored the impact of tablet position to further characterize the hydrodynamics within the device. Bocanegra et al. used Laser Doppler Anemometry to collect velocity measurements at selected fixed locations within the Apparatus II; however, the complete flow field and its mixing properties were not studied in detail (Bocanegra et al., 1990). The flow field and mixing characteristics of the USP Apparatus II are not well understood despite the data from previous work that suggests they strongly influence test results. The USP is currently evaluating potential changes to this test, and a comprehensive understanding of the hydrodynamics can provide significant contributions to aid in the evolution of this important tool.

In this paper, a computational model is used to aid in the understanding of the hydrodynamics controlling dissolution in the USP Apparatus II. The spatial distribution of the shear forces within the device are calculated from the simulated velocity field to show the direct impact of the hydrodynamics on the boundary layer for dissolution. Finally, targeted experiments are conducted to demonstrate the impact of non-uniform shear forces on dissolution measurements.

2. Materials and methods

2.1. Computational fluid dynamics (CFD)

CFD modeling of the dissolution apparatus in this investigation is performed using several software programs. Three-dimensional geometry specification and mesh generation are accomplished using ICEM-CFD (ICEM CFD Engineering, Berkeley, CA). An unstructured tetrahedral mesh of the device, consisting of 1.8 million first-order volumetric elements is developed and optimized. The commercially available AcuSolve program (ACUSIM software, Mountain View, CA) is used to solve the algebraic form of the Reynolds-Averaged Navier Stokes equations at each of the nodes defined by the mesh. This solver uses a Galerkin least-squares finite element formulation that provides second order accuracy. The code implements

[1] Reynolds number is traditionally defined as $Re = \rho ND^2/\mu$, where ρ is the fluid density, N the rotations per second of the agitator, D the agitator diameter, and μ is the fluid viscosity.

Table 1
CFD model parameter values

Parameter	Parameter value(s)
Mesh type	Unstructured, tetrahedral
Number of elements	1,843,609 tetrahedra
Number of nodes	330,117 nodes
Turbulence closure model	Spalart–Allmaras model
Model convergence criteria	Residuals $<1 \times 10^{-4}$
Fluid viscosity (cP)	1.0
Fluid density (kg/m^3)	1000
Agitation speed (rpm)	50–100

the Spalart–Allmaras closure model for turbulence modeling and requires all of the weighted residuals of the governing equations to converge to less than 10^{-4}. Table 1 details the relevant parameters for the model used in this work. Further technical details regarding the use of this CFD code for investigations of stirred tanks can be found elsewhere (Johnson and Bittorf, 2002). Particle tracking was accomplished using commercially available software provided by Acusim. Subsequent mixing analysis is performed using custom software developed at the Pharmaceutical Engineering Program at Rutgers University (Zalc, 2000; Zalc et al., 2001).

2.2. Planar laser induced fluorescence

Planar Laser Induced Fluorescence (pLIF) is a non-intrusive, visual technique that reveals the time evolution of a mixing process. Fig. 1(a) depicts the experimental set-up used for pLIF. Fluorescent dye is injected in a mixing system and illuminated with a planar laser so that mixing patterns created by the flow can be captured. The density of the dye must be properly matched to the density of the fluid to reveal the flow structures. Images of the illuminated plane are captured using a CCD camera to unveil the emerging mixing patterns. The convection of the dye tracer reveals well-mixed and poorly-mixed regions in the mixer. Convection carries dye rapidly to regions where mixing is good while segregated regions of the mixer remain dark for a long time since diffusion is the primary mechanism to bring dye into them. For the images reported in this work, a 32 mJ YAG laser (New Wave Research, Sunnyvale, CA) generates the laser sheet with a wavelength of 532 nm. Rhodamine WT (Exciton, Inc., Dayton, OH) is the fluorescent dye. A Dantec 80C42 Double Image 700 CCD camera (Dantec Dynamics, Mahwah, NJ) images the flow field with a 552 nm filter on the camera lens. The Flowmap software package with Flow Manager 4.0 (Dantec Dynamics, Mahwah, NJ) performs data acquisition and laser/camera synchronization.

2.3. Dissolution sampling studies

Dissolution sampling studies are performed using 220 mg Naproxen Sodium Tablets (CVS Pharmacy, Inc., Woonsocket, RI) purchased from a local pharmacy. The USP Paddle Method is followed using a standard 1-L dissolution vessel and 7.5 cm diameter paddle (SOTAX Corporation, Horsham, PA), assembled as per the USP 24 Physical Test section on dissolution (2000). The studies are conducted at ambient temperature using a pH 7.4 phosphate buffer. The tablet location is carefully controlled by preparing a circular ring on the inner dish of the dissolution vessel using silicone glue, 11 mm in diameter, in which the tablet could be placed. Two positions are tested; one in which the tablet is centered at the bottom of the vessel, the other in which the ring is positioned 21 mm from the center. The medium is agitated at 50 rpm for the duration of the test. Samples are manually removed from the vessel at 5 min intervals, beginning at $t = 0$ and ending at 45 min. At each time point, three 3-mL samples are removed; the first is taken from the top surface of the liquid media, the second from the middle region of the dissolution vessel (typically referred to as the sampling zone), and the last is removed from a location directly beside the paddle as depicted in Fig. 1(b). Immediately upon sampling, the contents are filtered using a 0.45 μm filter and stored in a parafilmed vial until analyzed. The volume of medium removed at each time point is not replaced as specified by the USP guidelines since the goal of these tests was solely to serve as a comparison between the various tablet positions. Three experiments are performed for each tablet position to establish reproducibility. The samples are analyzed by UV using a UV-1601 UV–vis Spectrophotometer (Shimadzu Corporation, Columbia, MD) at a wavelength of 332 nm. The percentage of drug dissolved at each time point can then be calculated, accounting for the volume of medium removed during sampling.

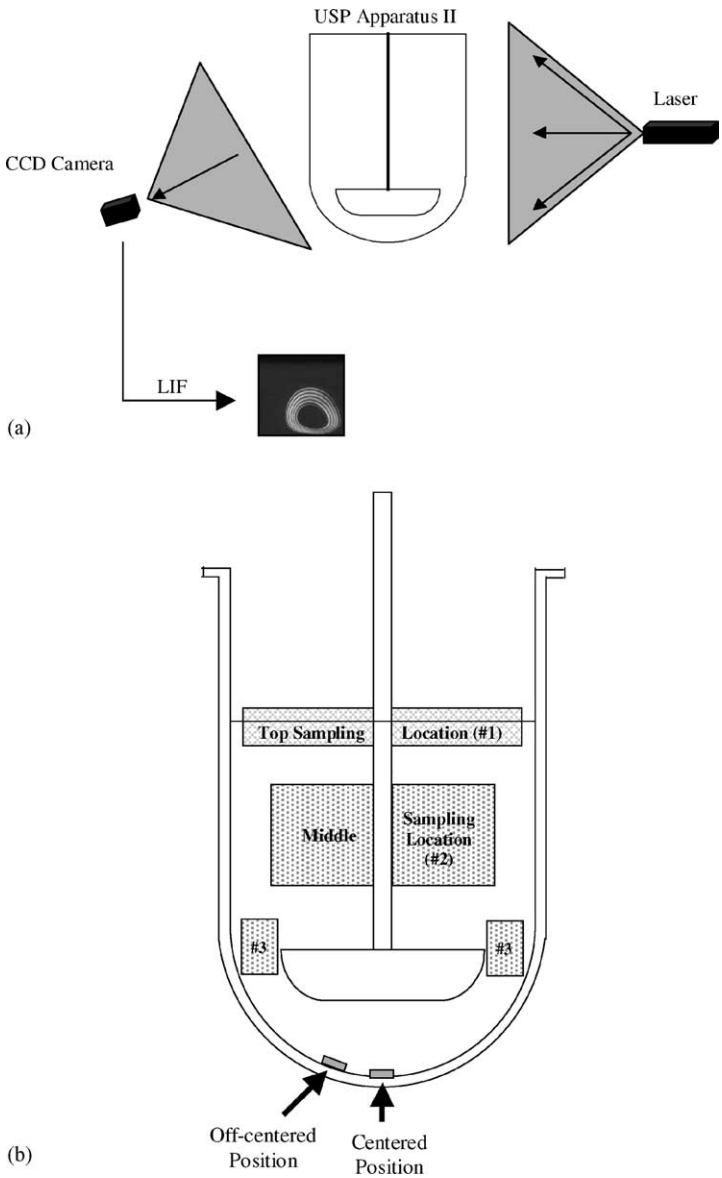

Fig. 1. Diagram of experimental set-up (a) and sampling locations (b).

3. Results

3.1. Turbulent velocity field

The instantaneous velocity field fluctuates rapidly for any flow in the turbulent regime. While computation of time-dependent flows is very involved, CFD can compute a time-averaged velocity field that predicts the mean flow under steady-state conditions. Fig. 2 presents time-averaged velocity fields in the plane of the paddle for two common operating conditions. Fig. 2(a) corresponds to mixing an aqueous solution at 50 rpm and the agitator velocity in Fig. 2(b) is 100 rpm. Each of the figures uses a different multiplier to scale the velocity vectors according to their magnitude. The time-averaged velocity field

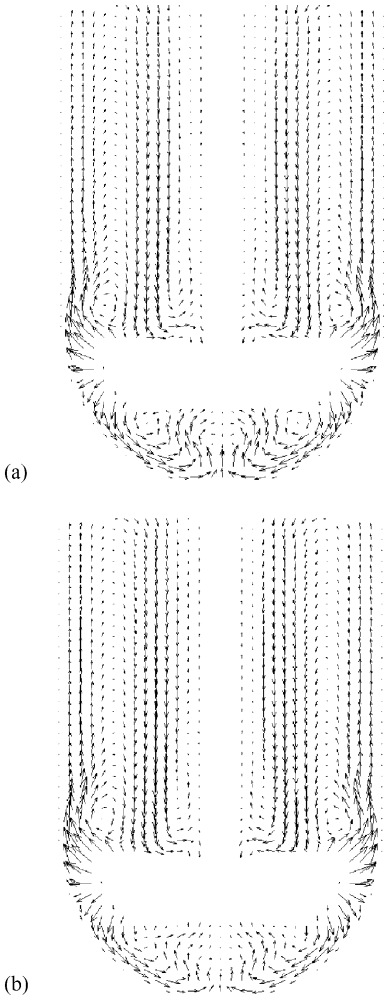

Fig. 2. Time-averaged velocity field at 50 rpm (a) and 100 rpm (b) in the plane of the impeller.

patterns are only slightly different at the two speeds. On average, material ejected from the impeller either moves up the wall to the top before returning down a channel midway between the shaft and wall, and fluid gets pushed down to the bottom along the wall before moving up to the impeller in the center of the device. Recirculating regions marking the secondary flow, first reported in this device by Bocanegra et al. (1990), exist both above and below the impeller. These velocity fields do not present significant new information regarding flow in the USP Apparatus II but provide the raw data for a mixing analysis.

3.2. Particle tracking

An analysis of hydrodynamic and mixing behavior requires more than simply the characterization of a velocity field. Velocity fields only indicate long-term recirculation zones in the flow and possible isolated "dead" zones, which is not adequate to describe short time mixing in a dynamic system. Flow visualization experiments and simulations facilitate analysis of mixing phenomena. Carefully conducted dye advection experiments unveil flow patterns and coherent structures that serve as the starting point to analyze fluid mixing. Dye advection experiments use a neutrally buoyant dye such that the tracer moves with the identical velocity of the fluid, and simulations can track massless particles that follow the flow in the same manner. A description of the mixing process is then assessed by examining the location of tracers as a function of space and time.

Fig. 3(a) shows a picture from a pLIF experiment conducted with an aqueous solution at 50 rpm. The image is a negative of the original photograph and shows the location of the dye as gray and black regions on the white background. The picture was taken a few seconds after injecting the dye above the paddle blade. Consistent with the velocity field shown in Fig. 2, the dye travels quickly up the wall above the impeller and later fills the region immediately surrounding the shaft. The dye is also transported to a small region below the

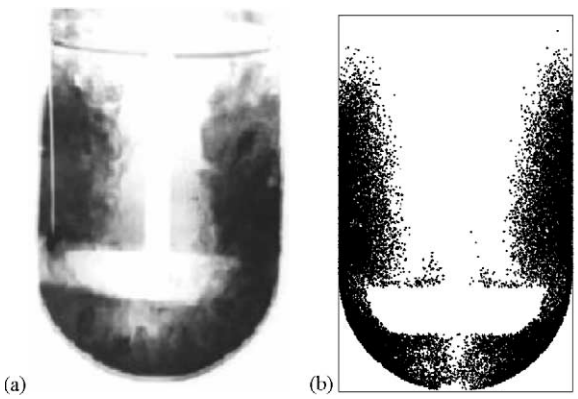

Fig. 3. Mixing patterns at 50 rpm revealed with an experiment using a neutrally buoyant dye (a) and computational particle tracking (b).

center of the paddle more slowly than the outer areas. Similar trends are identified with the results of particle tracking simulations in Fig. 3(b). The initial condition of the particle tracking is a sphere of points placed in a location similar to the point of injection of the dye in the experiment depicted in Fig. 3(a). Whenever a particle crosses the plane parallel with the agitator blade at the center of the vessel, the particle-tracking algorithm plots its position. All of the intersections made during the first 6 s of mixing are shown in Fig. 3(b). Similar to the pLIF experiments, the particles initially fill the outside of the tank before invading the regions near the shaft and immediately below the center of the paddle. The reasonable comparison of Fig. 3(a) and (b) provides confidence that the CFD model is accurately capturing mixing features within the device.

The mixing patterns in Fig. 3 do not show a distinct structure or the repeated, folding mixing pattern that was found in a study of the hydrodynamics in the laminar regime within the USP paddle device (Kukura et al., 2003). Turbulent fluctuations generally prevent the formation of such large-scale patterns since the mechanism of transport is accomplished via the transport of momentum and energy through eddies of different length scales. However, the efficient dispersion of tracers via turbulence does not imply that material in the apparatus experiences a uniform hydrodynamic environment. The following section will examine the range of fluid forces that the flow field exerts on dosage forms moving within the mixer.

3.3. Strain distribution

A physically relevant quantity to many dissolution tests that can be extracted from the CFD velocity fields but would be difficult to measure experimentally is the strain (or deformation) rate of the fluid. This measure is directly related to the shear force exerted by the fluid motion. In the context of dissolution, the magnitude of the strain rate controls the boundary layer thickness of fluid at the surface of the tablet that influences the mass transfer of material from the dosage form into the bulk fluid. High strain rates lead to thinner boundary layers, promoting faster transport. If transport through this layer is a limiting factor in dissolution, then high variability in strain rates has the potential to lead to inconsistent dissolution performance. Experiments have shown that variation in the boundary layer thickness

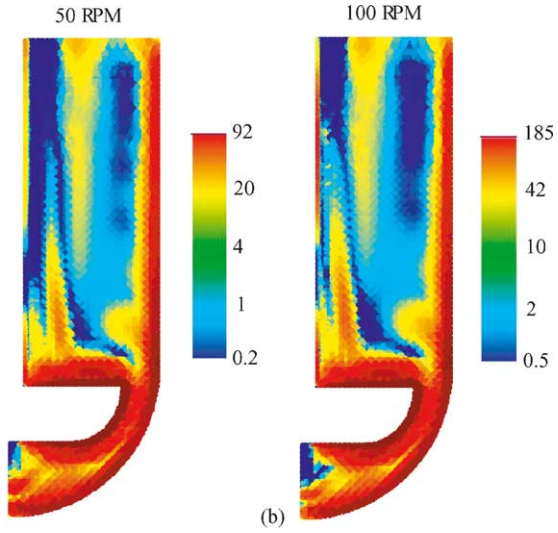

Fig. 4. Distribution of strain rates within the media at 50 rpm (a) and 100 rpm (b).

due to changing agitation speeds can compromise the ability of the in vitro test to predict in vivo performance (Hamlin et al., 1962). Fig. 4 shows the distribution of strain rates in the plane of the impeller at agitator speeds of 50 and 100 rpm. The contour plots show that the pattern at 50 rpm (Fig. 4(a)) is comparable to the distribution observed at 100 rpm, but at roughly half the scale. Changing the agitator speed in this range affects the magnitude but not the spatial distribution of strain rates. In both cases, the highest shear exists at the surface of the impeller. The vessel wall also experiences high deformation relative to the interior of the tank. The lowest shear is found between the shaft and wall above the impeller. Increasing the agitator speed increases the intensity of fluid forces but does not improve the homogeneity of the dissolution environment.

The heterogeneity of the shear forces is especially significant along the vessel wall and bottom surface where a tablet is most likely to rest. Fig. 5(a) and (b) show the instantaneous strain distribution along the wall at 50 rpm when viewed from the side and bottom, respectively. Corresponding images for 100 rpm are presented in Fig. 5(c) and (d). Similar to Fig. 4, the contour fields have similar distributions with the magnitudes of values at 50 rpm being half those at 100 rpm. The most striking observation from Figs. 4 and 5 is the presence of a circular low-shear region at

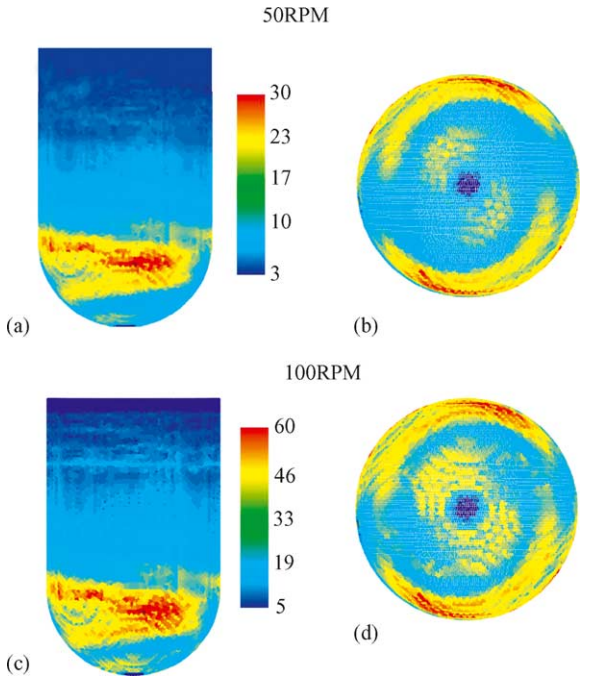

Fig. 5. Distribution of strain rates along the vessel surface at 50 rpm (a and b) and 100 rpm (c and d).

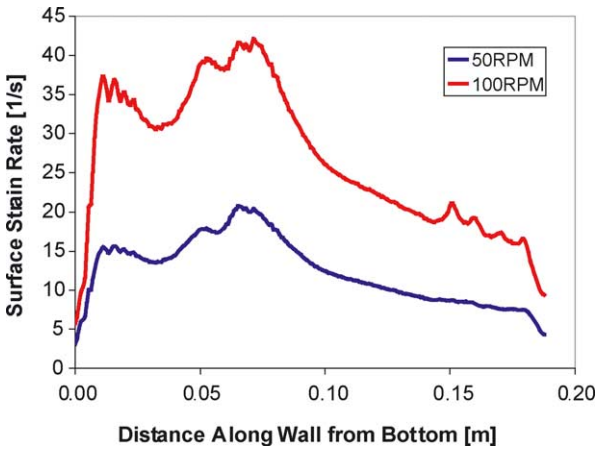

Fig. 6. Average strain rate along the wall as a function of distance from the bottom.

the center of the bottom of the device. This region is approximately the size of a typical dosage form. Outside of that small area, the shear forces rise rapidly.

Upon taking the azimuthal average of the contour plots in Fig. 5, the shear as a function of radial position can be calculated for each rotational speed. Fig. 6 shows the average strain rate as a function of distance (along the wall) from the bottom of the dish. The data corresponds to paddle speeds of 50 and 100 rpm. The graph depicts a steep change in shear intensity that a tablet might experience if moved, even slightly, from the center of the dish. This dramatic change in shear intensity can have detrimental effects on the experimentally measured dissolution rates. The highest shear rates along the wall are observed at the height of the impeller and the intensity slowly decays along the wall.

3.4. Dissolution sampling experiments

Experiments that measure and compare the dissolution rates of tablets at various locations within the USP Apparatus II demonstrate the impact that non-uniform shear forces can have on dissolution measurements. Fig. 7(a) shows a plot of the percent of drug dissolved versus time for the Naproxen Sodium tablets at two tablet locations.[2] The measured dissolution rates are substantially lower for the tablets placed in the centered position than those observed for the case of the off-centered tablets. Upon comparing these data to the graph in Fig. 7(b), the cause of these differences becomes apparent. The centered position corresponds to the initial starting location for the graph (distance = 0.00 m), circled with a solid gray line, while the off-centered position refers to a distance along the wall of approximately 0.02 m on the graph, denoted with a dashed gray circle. The shear forces exerted at the two tablet locations exhibit a three-fold difference. The impact of such a shear rate difference on dissolution is clearly evident in the experiments.

The effect of sampling location was also explored in these dissolution experiments. Results from the six experiments showed a slight trend in which samples removed from beside the paddle contain slightly higher concentrations of dissolved drug than those removed from the middle region, while samples removed from the top surface appear to contain the least amount of dissolved drug. However, the differences observed between the three sample locations were small (i.e. approximately 0.5% dissolved drug difference) and no true discernable difference can be attributed

[2] *Note*: The measurements from the three sample locations at each time point were averaged for the plot in Fig. 7(a).

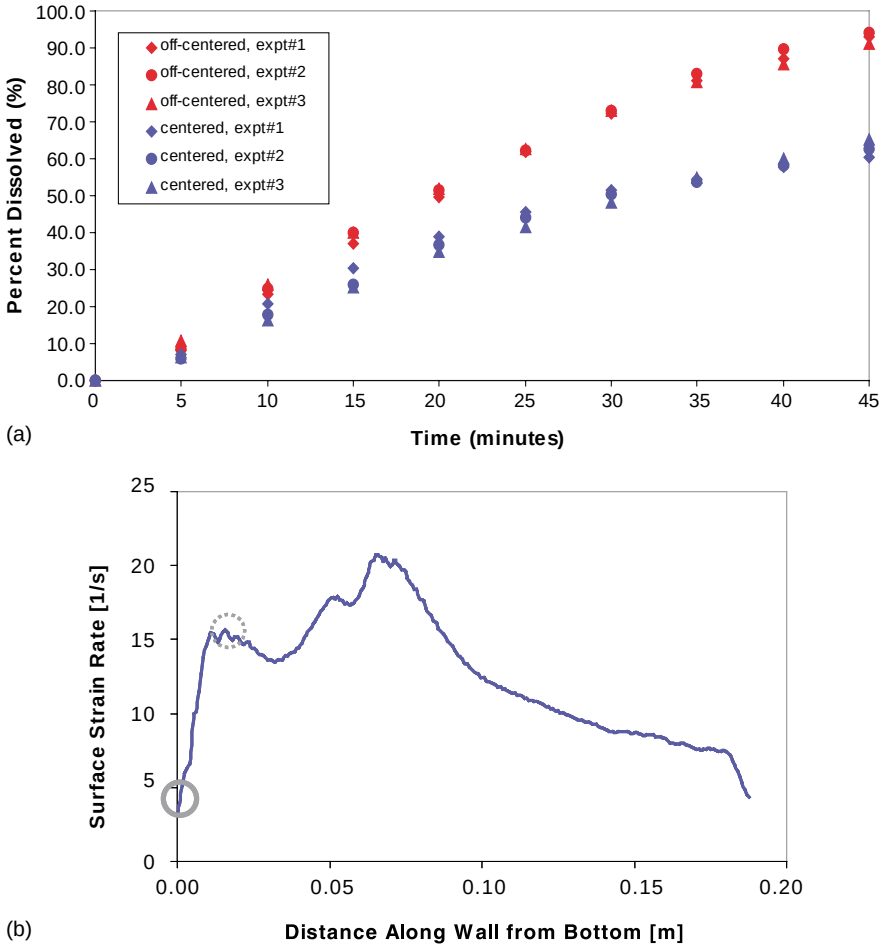

Fig. 7. Differing dissolution rates resulting from changes in tablet location (a) that have significantly different shear environments (b).

to insufficient mixing under the conditions of the experiment.

4. Discussion

This article uses CFD models to show that the shear strain environment in an aqueous media within the USP Apparatus II is highly heterogeneous. Changing the agitator speed from 50 to 100 rpm only increases the intensity of the shear force exerted by the fluid but it does not improve the homogeneity of the spatial distribution of shear. Experiments confirm that dissolution rates can vary substantially when tablets experience different shear environments due to their physical location within the device. These results aid in understanding the underlying hydrodynamics within the USP Apparatus II and demonstrate the impact that heterogeneity can have on dissolution measurements. These data help explain many of the problems typically encountered with dissolution testing in the USP Apparatus II. Lastly, the results demonstrate the predictive power of the CFD models.

The USP has recently discussed potential changes in dissolution testing, including operation in the laminar regime that may provide more uniform environments (USP Dissolution Meeting, January 2003). Evaluation of the dissolution environment in the manner demonstrated here will contribute important benefits to the

development of rigorous dissolution tests, potentially preventing many problems.

Acknowledgements

The authors wish to acknowledge the financial support of this project to the Schering-Plough Research Institute, Johnson and Johnson, Wyeth and to Merck & Co., Inc. for the support of Jennifer Baxter and Joseph Kukura during their doctoral studies.

References

Beckett, A.H., Quach, T.T., Kurs, G.S., 1996. Improved hydrodynamics for USP Apparatus 2. Diss. Tech. 3, 7–18.

Bocanegra, L.M., Morris, G.J., Jurewicz, J.T., Mauger, J.W., 1990. Fluid and particle laser doppler velocity measurements and mass transfer predictions for USP paddle method dissolution apparatus. Drug Dev. Ind. Pharm. 16, 1441–1462.

Cartensen, J., Lai, T.Y., Prasad, V.K., 1978. USP dissolution IV: comparison of methods. J. Pharm. Sci. 67, 1303–1307.

Costa, P., Lobo, J.M.S., 2001. Influence of dissolution medium agitation on release profiles of sustained-release tablets. Drug Dev. Ind. Pharm. 27, 811–817.

Cox, D.C., Furman, W.B., Thornton, L.K., Moore, T.W., Jefferson, E.H., 1983. Systematic error associated with Apparatus 2 of the USP dissolution test III: limitations of calibrators and the USP suitability test. J. Pharm. Sci. 72, 910–913.

Hamlin, W.E., Nelson, E., Ballard, B.E., Wagner, J.G., 1962. Loss of sensitivity in distinguishing real differences in dissolution rates due to increasing intensity of agitation. J. Pharm. Sci. 51, 432–435.

Johnson, K., Bittorf, K.J., 2002. Validating the galerkin least-squares finite element methods in predicting mixing flows in stirred tank reactors. In: Proceedings of the 10th Annual Conference of the CFD Society of Canada, Windsor, Ont., pp. 490–496.

Kukura, J., Arratia, P.C., Szalai, E.S., Muzzio, F.J., 2003. Engineering tools for understanding hydrodynamics of dissolution tests. Drug Dev. Ind. Pharm. 29, 231–239.

Levy, G., 1963. Effect of certain tablet formulation factors on dissolution rate of the active ingredient. J. Pharm. Sci. 52, 1039–1046.

Moore, T.W., Cox, D.C., Demarest, D.A., 1997. Dissolution calibrator tablets: a scaled-up lot of a new calibrator tablet recommended to replace both current USP calibrator tablets. Pharm. Forum 23, 5352–5359.

Moore, T.W., Hamilton, J.F., Kerner, C.M., 1995. Dissolution testing: limitations of the USP prednisone and salicylic acid calibrator tablets. Pharm. Forum 21, 1387–1396.

Morihara, M., Aoyagi, N., Kaniwa, N., Katori, N., Kojim, S., 2002. Hydrodynamic flows around tablets in different pharmacopeial dissolution tests. Drug Dev. Ind. Pharm. 28, 655–662.

Qureshi, S.A., Shabnam, J., 2001. Cause of high variability in drug dissolution testing and its impact on setting tolerances. Eur. J. Pharm. Sci. 12, 271–276.

The Gold Sheet, 2000. Drug Product Recalls Spiked in 1999, vol. 34, F-D-C Reports, Inc., Maryland, pp. 1–15.

The Gold Sheet, 2001. Drug Recall Data for 2000, vol. 35, F-D-C Reports, Inc., Maryland, pp. 1–19.

Underwood, F., Cadwallder, D., 1976. Effects of various hydrodynamic conditions on dissolution rate determinations. J. Pharm. Sci. 65, 697–700.

US Pharmacopeia XXIV, 2000. US Pharmacopeial Convention, Rockville, MD.

Vongvirat, B., Howard, S.A., Mauger, J.W., Luzzi, L.A., 1981. Design and evaluation of a rotating filter-magnetic basket apparatus: tablet and basket position. Int. J. Pharm. 9, 199–211.

Wells, C., 1981. Effect of sampling probe size on dissolution of tableted drug samples. J. Pharm. Sci. 70, 232–233.

Zalc, J.M., 2000. Computational Fluid Dynamics (CFD) Tools for Investigating Flow and Mixing in Industrial Systems: The Koch-Glitsch SMX Static Mixer and a Three Rushton Turbine Stirred Tank. Ph.D. Thesis, Department of Chemical and Biochemical Engineering, Rutgers University, New Brunswick, NJ.

Zalc, J.M., Alvarez, M.M., Muzzio, F.J., 2001. Extensive validation of computed laminar flow in a stirred tank with three Rushton turbines. AIChE J. 47, 2144–2154.